ISSN 1070-3284, Russian Journal of Coordination Chemistry, 2014, Vol. 40, No. 3, pp. 149–153. © Pleiades Publishing, Ltd., 2014.

A New 2D Mn(II) Coordination Polymer Constructed from Carboxylate and N-Donor Coligand: Synthesis, Structure, and Magnetism[1]

J. Wang[a, b, c, *], L. Lu[a, b], W. P. Wu[a, b], L. K. Zou[a, b], and B. Xie[a, b]

[a] *Institute of Functionalized Materials, Sichuan University of Science & Engineering, Zigong, 643000 P.R. China*

[b] *School of Chemistry and Pharmaceutical Engineering, Sichuan University of Science & Engineering, Zigong, 643000 P.R. China*

[c] *Key Laboratory of Synthetic and Natural Functional Molecule Chemistry of the Ministry of Education, Shanxi Key Laboratory of Physico-Inorganic Chemistry, College of Chemistry and Materials Science, Northwest University, Xi'an, 710069 P.R. China*

**e-mail: scwangjun2011@126.com*

Received October 29, 2012

Abstract—A new complexes, namely, $\{[Mn_2(L)_2(Bipy)_2] \cdot H_2O\}_n$ (**I**) (H_2L = diphenic acid, Bipy = 4,4'-bipyridine) has been synthesized and structurally characterized by single-crystal diffraction analysis. In **I**, the two *syn, anti*-carboxylate groups in L bridge Mn(II) forming a one-dimensional chain, which is further connected by Bipy into 2D double layer. Magnetic study reveals the overall antiferromagnetic interaction between neighboring Mn^{2+} ions in compound **I**.

DOI: 10.1134/S1070328414030099

INTRODUCTION

Over past decades, the field of crystal engineering has achieved significant success in developing a variety of metal-organic frameworks [1–3]. The interest arises not only from their versatile fascinating architectures but also from their promising applications [4]. Many works have been devoted to the selection or design of suitable ligands containing certain features. Among the reported studies, organic ligands with carboxylate groups are of especial interest because they can adopt a variety of coordination modes and result in diverse multidimensional frameworks [5–11]. H_2L is utilized as multifunctional ligand owing to their high coordination numbers and modulating coordination environments [12]. Two ionizable hydrogen atoms can be partially or completely deprotonated to generate L anion. Moreover, H_2L has a C–C single bond between two phenyl rings to form skew coordination orientation of the carboxylate groups [13, 14]. To date, some Cu/Cd coordination polymers with diphenic acid ligand have been reported [15]. However, a few Mn(III) complexes of diphenic acid ligand have been studied.

On the other hand, 4,4'-bipyridine (Bipy) or a combination with other ligands can be used for the construction of intriguing supramolecular motifs using covalent coordination and hydrogen bonds to give one-dimensional structures and higher-dimensional coordination polymers [16]. With this background in mind, we chose diphenic acid (H_2L) as a organic ligand to react with the Mn^{2+} ion in the presence of rigid N-donor (Bipy). A new polymer $\{[Mn_2(L)_2(Bipy)_2] \cdot H_2O\}_n$ (**I**) was obtained under mild condition. In **I**, the two *syn, anti*-carboxylate groups in L bridge Mn(II) forming a one-dimensional chain, which is further connected by Bipy into 2D double layer. Magnetic study reveals the overall antiferromagnetic interaction between neighboring Mn^{2+} ions in compound **I**.

EXPERIMENTAL

Materials and physical measurements. All the reagents and solvents for synthesis and analysis were commercially available and used directly. Elemental analyses for carbon, hydrogen and nitrogen were performed on a Vario EL III elemental analyzer. The infrared spectra (4000–600 cm^{-1}) were recorded by using KBr pellet on an AVATAR-370 (Nicolet) IR spectrometer. The crystal determination was performed on a Bruker SMART APEX II CCD diffractometer equipped with graphite-monochromatized MoK_α radiation (λ = 0.71073 Å). TGA were carried out with a Metter–Toledo TA 50 in dry dinitrogen (60 mL min^{-1}) at a heating rate of 5°C min^{-1}. X-ray power diffraction (XRPD) data were recorded on a Rigaku RU200 diffractometer at 60 KV, 300 mA for CuK_α radiation (λ = 1.5406 Å), with a scan speed of 2°C/min and a step size of 0.02° in 2θ. Magnetic susceptibility data of

[1] The article is published in the original.

Table 1. Crystal data and structure refinement information for compound ***I***

Parameter	Value
Formula weight	920.67
Crystal system	Orthorhombic
Space group	$Pna2_1$
a, Å	17.791(7)
b, Å	23.255(9)
c, Å	9.833(4)
V, Å^3	4068(3)
Z	4
ρ_{calcd}, g/cm^3	1.503
μ, mm^{-1}	0.687
$F(000)$	1888
θ Range, deg	2.28–26.30
Limiting indices h, k, l	$0 \le h \le 18$, $0 \le k \le 26$, $0 \le l \le 8$
Reflection collected	16952
Independent reflections (R_{int})	4904 (0.0848)
Reflections with $I > 2\sigma(I)$	3608
Number of parameters	575
Goodness-of-fit	1.041
R_1, wR_2 ($I > 2\sigma(I)$)*	0.0701, 0.1617
R_1, wR_2 (all data)**	0.1065, 0.1915
$\Delta\rho_{min}/\Delta\rho_{max}$, e Å^{-3}	0.098

* $R = \Sigma(F_o - F_c)/\Sigma(F_o)$, ** $wR_2 = \{\Sigma[w(F_o^2 - F_c^2)^2]/\Sigma(F_o^2)^2\}^{1/2}$.

powdered samples restrained in parafilm were measured on Oxford Maglab 2000 magnetic measurement system in the temperature range 300–1.8 K and at field of 1 KOe.

X-ray crystallography. Single crystal X-ray diffraction analyses of the compound was carried out on a Bruker SMART APEX II CCD diffractometer equipped with a graphite monochromated MoK_α radiation (λ = 0.71073 Å) by using φ/ω scan technique at room temperature. The intensities were corrected for Lorentz and polarization effects as well as for empirical absorption based on multi-scan techniques; all structures were solved by direct methods and refined by full-matrix least-squares fitting on F^2 by SHELX-97 [17]. Absorption corrections were applied by using multi-scan program SADABS. The hydrogen atoms of organic ligands were placed in calculated positions and refined using a riding on attached atoms with isotropic thermal parameters 1.2 times those of their carrier atoms. The water hydrogen atoms were located from difference maps and refined with isotropic thermal parameters 1.5 times those of their carrier atoms. Table 1 shows crystallographic data of **I**. Selected bond distances and bond angles, parameters are listed in Table 2. Supplementary material for structure **I** has been deposited with the Cambridge Crystallographic Data Centre (no. 902918; deposit@ccdc.cam.ac.uk or http://www.ccdc.cam.ac.uk).

Synthesis of complex I. A mixture of H_2O (8 mL) and CH_3OH (8 mL) solution containing H_2L (0.1 mmol) and Bipy (0.1 mmol) was added $Mn(OAc) \cdot 2H_2O$ (0.12 mmol) in water at 80°C. The pH of the resulting solution was adjusted to 7 using dilute NaOH (0.1 mol/L) and kept at room temperature to prepare compound **I**. From that solution, pale yellow crystals suitable for X-ray measurements were obtained. The yield was 50%.

For $C_{48}H_{34}N_4O_9Mn_2$ (M = 920.67)

anal. calcd., %:	C, 62.62;	N, 6.09;	H, 3.72.
Found, %:	C, 62.55;	N, 6.21;	H, 3.50.

IR (KBr; ν, cm^{-1}): 3421 v.s, 2992 m, 1618 v.s, 1502 m, 1488 v.s, 1255 v.s, 1185 s, 1012 m, 955 m, 887 m,752 m.

RESULTS AND DISCUSSION

The results of crystallographic analysis revealed that the asymmetric unit of complex **I** contains two crystallographically unique Mn(II) atom, two L and two Bipy ligands and one coordinative water molecule. As shown in Fig. 1, Mn(1) and Mn(2) have the same coordination geometries, which are completed by four oxygen atoms from four different L ligands (η^1-η^1-μ_2) and two N atoms from two Bipy molecules. The Mn–O and Mn–N distances are in the normal ranges (Table 2). The L has *S*- and *R*-configuration enantiomorph (Fig. 2). In complex **I**, the L ligands just act as the gemel, connecting the dinuclear SBUs into a chain structure along the *y* axis (Fig. 2). The *S*- and *R*-ligands are at each side of the chain. The phenyl rings of L are not coplanar, with the dihedral angle of 76.5°. The combination of these twisting allows L to link Mn(II) centers into a one-dimensional chain containing repeated eight-membered (–Mn–O–C–O–) rings (Fig. 2a) [13, 14]. The Mn···Mn separation in the rings is 5.069 Å. There are no other short contacts and noteworthy weak interactions between the adjacent chains. Complex **I** is a two-dimensional layer structure consisting of one-dimensional L–Mn chains bridged by Bipy. There are two independent L ligands in asymmetric unit, both of them behave in a bis-bidentate fashion through two *syn*, *anti*-carboxylate groups bridging three Mn(II) (Fig. 3).

As to FT-IR spectra, the compouns show a broad band centered around 3421 cm^{-1} attributable to the

O–H stretching frequency of the water cluster. The O–H stretching vibration for *Ic* appears as a broad band centered around 3200 cm^{-1}. Specifically, asymmetric stretching vibration ν(COO^-) and the symmetric stretching vibration ν(COO^-) are observed 1618 and 1488 cm^{-1}, respectively. For that, the difference between the asymmetric and symmetric stretches, $\Delta\nu_{as}(COO^-)-\nu_s(COO^-)$, are on the order of 150 cm^{-1} indicating that carboxyl groups are coordinated to the metal in a bidentate modes [18], consistent with the observed X-ray crystal structure of **I**.

To study the stability of the polymer, thermogravimetric analyses (TGA) of complex **I** was performed (Fig. 4). The TGA diagram of **I** shows two weight loss steps. The first weight loss began at 35°C and completed at 165°C. The observed weight loss of 2.1% is corresponding to the loss of the water molecule (calcd. 1.9%). The second weight loss occurs in the range 186–408°C, which can be attributed to the elimination of L and Bipy ligands.

Additionally, to confirm the phase purity of compound **I**, the original sample was characterized by XRPD method. Although the experimental patterns have few unindexed diffractions lines and some are slightly broadened in comparison to those simulated from single-crystal models, it can still to be considered that the bulk synthesized materials and as-grown crystal are homogeneous for compound **I**.

The variable-temperature magnetic susceptibility was measured from 2 to 300 K at 1000 Oe for **I**. The magnetic data of **I** is displayed in Fig. 5a, plotted as thermal variation of $\chi_M T$ and χ_M. The $\chi_M T$ vs. T plot has a value of 9.06 $cm^3\ mol^{-1}$ K, which is little larger than the spin-only value (8.76 $cm^3\ mol^{-1}$ K) for $S = 5/2$ per formula unit in **I** [19]. As the temperature was lowered, the $\chi_M T$ values decreased, typical of antiferromagnetic behavior. And the compound shows the Curie–Weiss behavior in the whole temperature region of measurement (Fig. 5b) with the Curie and Weiss constants being $C = 8.29$ emu mol^{-1} K and $\theta = -0.35$ K, respectively. Thus, the temperature dependences of the magnetic susceptibility of **I** was modeled with theoretical expression deduced from the spin Hamiltonian $\hat{H} = -2J\sum_{i=j}\hat{S}_i\hat{S}_j$ ($S = 5/2$), and modified to include an amount of uncoupled species. The most appropriate fit is the result of Mn(II) dimeric system (Eq. 1), which the dominant magnetic interactions is the isotropic interaction involving the two local doublet states of the Mn^{2+} ions that form the dimmers [20].

$$\chi_d = \frac{Ng^2\beta}{3KT}\frac{55 + 30e^{11\chi} + 14e^{10\chi} + 5e^{24\chi} + e^{28\chi}}{11 + 9e^{10\chi} + 7e^{18\chi} + 5e^{24\chi} + 3e^{28\chi} + e^{30\varphi}}.$$

With $\chi = -\frac{J^1}{KT}$ and J^1 is the intra-dimer coupling constant. Then the dimeric Mn(II) unit is taken as effective classical spin system with

Table 2. Selected bond distances (Å) and angles (deg) of structure **I**

Bond	d, Å	Bond	d, Å
Mn(1)–N(4)	2.316(7)	Mn(1)–N(2)	2.320(7)
Mn(1)–O(7)	2.179(7)	Mn(1)–O(1)	2.141(8)
Mn(1)–O(4)	2.154(7)	Mn(1)–O(6)	2.184(8)
Mn(2)–O(3)	2.151(7)	Mn(2)–O(2)	2.165(7)
Mn(2)–O(8)	2.189(8)	Mn(2)–O(5)	2.193(7)
Mn(2)–N(1)	2.311(6)	Mn(2)–N(3)	2.313(7)
Angle	ω, deg	Angle	ω, deg
O(1)Mn(1)O(4)	88.4(2)	O(4)Mn(1)O(6)	170.5(2)
O(1)Mn(1)O(7)	179.1(3)	O(4)Mn(1)O(7)	92.5(3)
O(1)Mn(1)O(6)	86.1(3)	O(7)Mn(1)O(6)	93.1(2)
O(1)Mn(1)N(4)	85.4(3)	O(4)Mn(1)N(4)	90.8(3)
O(7)Mn(1)N(4)	94.8(3)	O(6)Mn(1)N(4)	81.1(3)
O(1)Mn(1)N(2)	97.3(3)	O(4)Mn(1)N(2)	86.2(3)
O(7)Mn(1)N(2)	82.5(3)	O(6)Mn(1)N(2)	102.1(3)
N(4)Mn(1)N(2)	175.9(5)	O(3)Mn(2)O(2)	97.7(2)
O(3)Mn(2)O(8)	91.5(3)	O(2)Mn(2)O(8)	168.9(3)
O(3)Mn(2)O(5)	175.7(3)	O(2)Mn(2)O(5)	84.6(3)
O(8)Mn(2)O(5)	86.6(2)	O(3)Mn(2)N(1)	81.7(3)
O(2)Mn(2)N(1)	101.3(3)	O(8)Mn(2)N(1)	86.0(3)
O(5)Mn(2)N(1)	94.3(3)	O(3)Mn(2)N(3)	98.3(3)
O(2)Mn(2)N(3)	83.9(3)	O(8)Mn(2)N(3)	88.7(3)
O(5)Mn(2)N(3)	85.5(3)	N(1)Mn(2)N(3)	174.7(4)

$S_d = \left\{-1 + \left[1 + \frac{4\chi_d}{0.125g^2}\right]^{1/2}\right\}^2$. According to Fisher's model, the total magnetic susceptibility is

$$\chi_{chain} = \frac{Ng^2\beta S_d(S_d+1)}{3KT}\frac{1-\mu}{1+\mu},$$

$$\mu = \coth\left[\frac{2J_2S_d(S_d+1)}{KT}\right] - \frac{KT}{2J_2S_d(S_d+1)}.$$

The simulations leads to $J^1 = -0.28$ cm^{-1}, $J^2 = -3.22$ cm^{-1}, $g = 2.08$, as shown in Fig. 5a.

ACKNOWLEDGMENTS

The authors acknowledge financial assistance from Sichuan University of Science and Engineering, the

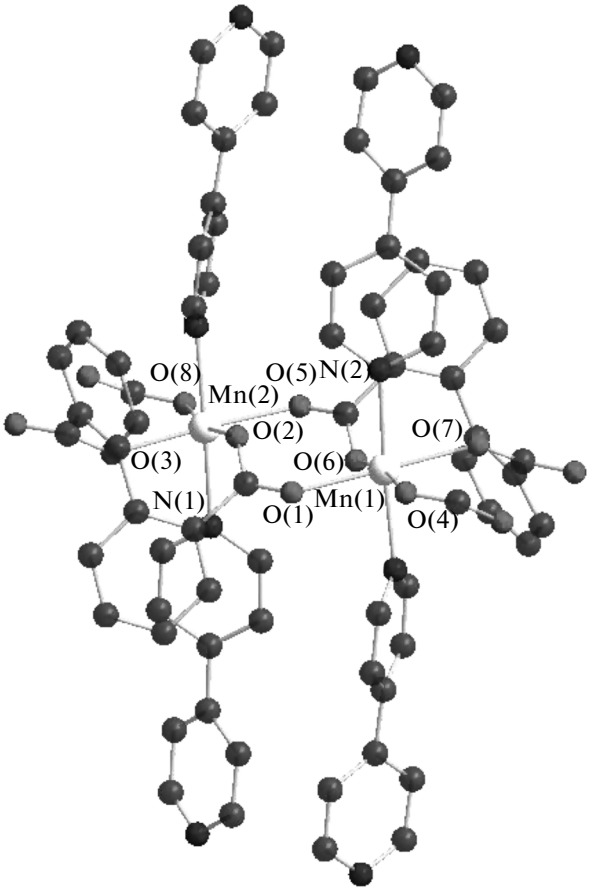

Fig. 1. View of the asymmetric unit of complex **I**.

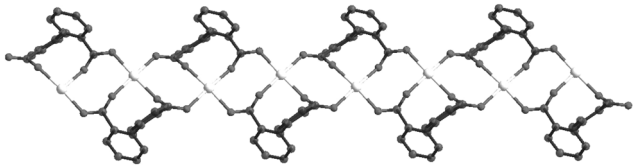

Fig. 2. View of the 1D chain directed by Mn^{2+} ions and L ligands in **I**.

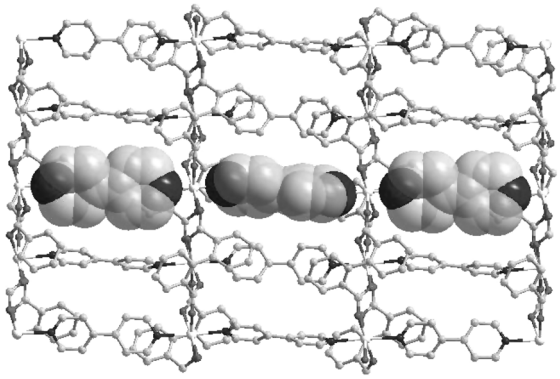

Fig. 3. View of the 2D gird network.

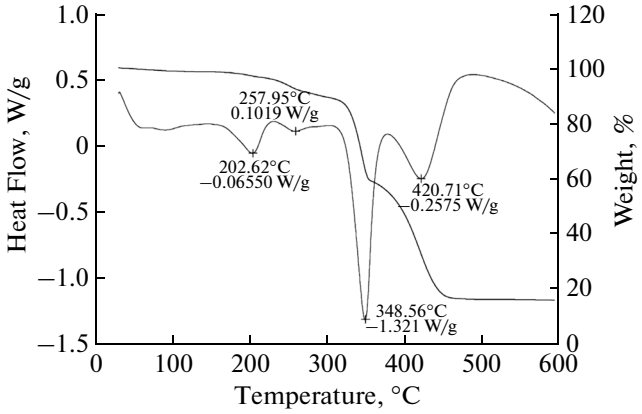

Fig. 4. TGA curve for compound **I**.

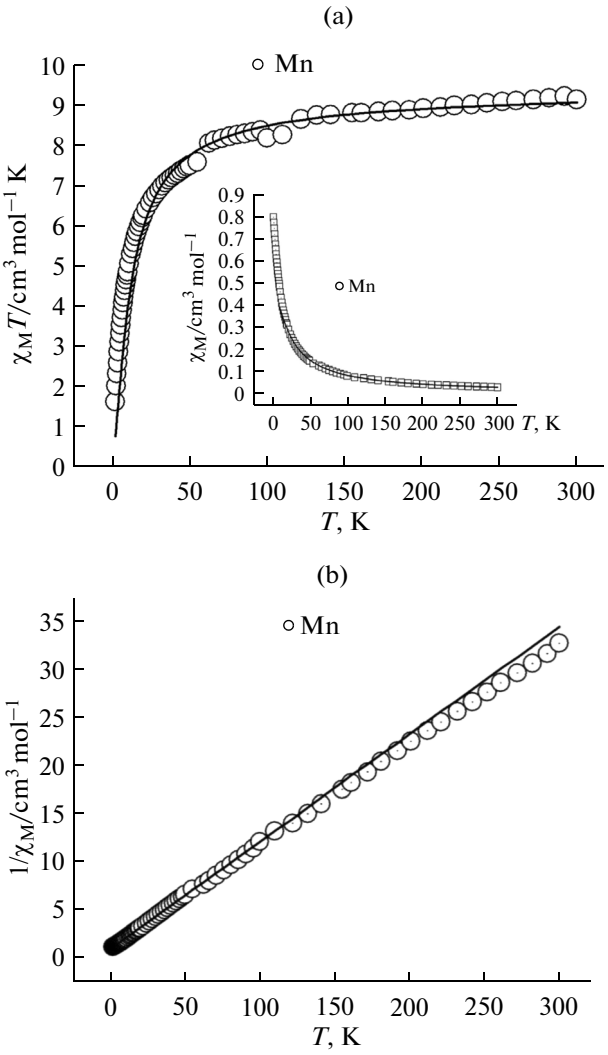

Fig. 5. Plots $\chi_M T$, χ_M (a) and $1/\chi_M$ (b) vs. T for **I**, solid lines represent fits to the data.

Institute of Functionalized Materials (nos. 2011KY02, 2012KY12, and 2010XJKYL005), the Opening Project of Key Laboratory of Green Catalysis of Sichuan Institutes of High Education (no. LYJ1207), and the Education Committee of Sichuan Province (nos. 12ZA090, 13ZB0131).

REFERENCES

1. Liu, K., Cruzan, J.D., and Saykally, R.J., *Science*, 1996, vol. 271, p. 929.
2. Sun, D., Xu, H.-R., Yang, C.-F., et al., *Cryst. Growth Des*., 2010, vol. 10, p. 4642.
3. Armentano, D., DeMunno, G., Faus, J., et al., *Inorg. Chem*., 2001, vol. 40, p. 655.
4. Lippert, B. and Miguel, P.J., *Chem. Soc. Rev*., 2011, vol. 40, p. 4475.
5. Atwood, J.L., Barbour, L.J., Ness, T.J., et al., *J. Am. Chem. Soc*., 2001, vol. 123, p. 7192.
6. Liu, J.Q., Huang, Y.S., Zhao, Y.Y., and Jia, Z.B., *Cryst. Growth Des*., 2011, vol. 11, p. 569.
7. Liu, J.Q., Wang, Y.Y., and Huang, Y.S., *CrystEngComm*, 2011, vol. 13, p. 3733.
8. Liu, J.Q., Wang, Y.Y., Wu, T., and Wu, J., *CrystEngComm*, 2012, vol. 14, p. 2906.
9. Liu, J.Q., Wang, Y.Y., Batten, S.R., et al., *Inorg. Chem. Commun*., 2012, vol. 19, p. 27.
10. Liu, J.Q., Wu, J., Wang, Y.Y., and Ma, D.Y., *J. Coord. Chem*., 2012, vol. 65, p. 1303.
11. Wu, J., Liu, J.Q., Wang, Y.Y., et al., *Inorg. Chem. Commun*., 2012, vol. 25, p. 10.
12. Zhang, H.J., Fan, R.Q., Zhou, G.P., et al., *Inorg. Chem. Commun*., 2012, vol. 16, p. 100.
13. Liu, Y., Qi, Y., Su, Y.H., et al., *CrystEngComm*, 2010, vol. 12, p. 3283.
14. Yi, X.Y., Yin, P.Y., Tong, L., et al., *Inorg. Chem. Commun*., 2011, vol. 14, p. 247.
15. Lu, J.Y. and Schauss, V., *Inorg. Chem. Commun*., 2003, vol. 6, p. 1332.
16. Wang, Z.L., Rong, L., and Wang, J.P., *Z. Naturforsch*., *B*, 2007, vol. 62, p. 1487.
17. Sheldrick, G.M., *SHELXL-97, Program for X-ray Crystal Structure Refinement*, Göttingen (Germany): Univ. of Göttingen, 1997.
18. Nakamoto, K., *Infrared and Raman Spectra of Inorganic and Coordination Compounds*, New York: Wiley Interscience, 1997.
19. Zhang, Y.N., Liu, J.Q., Wang, T., et al., *J. Mol. Struct*., 2006, vol. 878, p. 116.
20. Zheng, S., Meng, X.H., Zhou, Z.G., et al., *Inorg. Chem. Commun*., 2012, vol. 23, p. 31.